Advances in Applied Mathematics and Mechanics
Adv. Appl. Math. Mech., Vol. **1**, No. 1, pp. 89-106 (2009)

February 2009

Assessment of Timoshenko Beam Models for Vibrational Behavior of Single-Walled Carbon Nanotubes using Molecular Dynamics

Y. Y. Zhang[1], C. M. Wang[2,*] and V. B. C. Tan[1]

[1] *Department of Mechanical Engineering, National University of Singapore, Kent Ridge, Singapore 119260.*

[2] *Engineering Science Programme and Department of Civil Engineering, National University of Singapore, Kent Ridge, Singapore 117574.*

Received 15 October 2008 ; Accepted (in revised version) 2 December 2008

Available online 16 February 2009

Abstract. In this paper, we study the flexural vibration behavior of single-walled carbon nanotubes (SWCNTs) for the assessment of Timoshenko beam models. Extensive molecular dynamics (MD) simulations based on second-generation reactive empirical bond-order (REBO) potential and Timoshenko beam modeling are performed to determine the vibration frequencies for SWCNTs with various length-to-diameter ratios, boundary conditions, chiral angles and initial strain. The effectiveness of the local and nonlocal Timoshenko beam models in the vibration analysis is assessed using the vibration frequencies of MD simulations as the benchmark. It is shown herein that the Timoshenko beam models with properly chosen parameters are applicable for the vibration analysis of SWCNTs. The simulation results show that the fundamental frequencies are independent of the chiral angles, but the chirality has an appreciable effect on higher vibration frequencies. The SWCNTs is very sensitive to the initial strain even if the strain is extremely small.

AMS subject classifications: 74H45

Key words: Vibration, carbon nanotubes, molecular dynamics, Timoshenko beam models.

1 Introduction

In recent years, carbon nanotubes (CNTs) have triggered intensive studies to fulfill their potential applications in a variety of fields due to their exceptional mechanical, electronic and chemical properties. Their high stiffness and strength, low density

*Corresponding author.
URL: `http://www.eng.nus.edu.sg/civil/people/cvewcm/wcm.html`
Email: `mpezyy@nus.edu.sg` (Y. Y. Zhang), `cvewcm@nus.edu.sg` (C. M. Wang), `mpetanbc@nus.edu.sg` (V. B. C. Tan)

and good conductivity have made CNTs the foundation building element for nano-electromechanical devices [1–7]. One of the promising applications is the CNT-based unltrasensitive sensor. CNTs, in particular single-walled CNTs (SWCNTs), are small in size with large surface, stable in harsh chemical environment [5] and can respond to the external mechanical deformation rapidly with high sensitivity. In view of this, it is of great significance to gain a full understanding of the vibration properties of SWCNTs.

Vibration is one of the fundamental mechanical behaviors of CNTs. The vibration frequencies of CNTs have been employed in the determination of the Young's modulus of CNTs [1–4]. In the experiments conducted by Treacy et al. [1] and Poncharal et al. [3], clamped-free multi-walled CNTs (MWCNTs) excited by thermal or electrical loads were observed in a transmission electron microscope (TEM) for the resonance frequency. The frequency equation of a vibrating Euler beam is then used to obtain the Young's modulus in a reverse manner. Molecular dynamics (MD) have also been preformed on the thermal vibration of SWCNTs for the natural frequencies to predict the Young's modulus [4].

When compared with the extensive investigations of buckling or tensile behaviors of CNTs under axial loadings [6–12] relatively fewer studies have been done to analyze the vibration behaviors of CNTs. Similar to the buckling analysis of CNTs, the vibration behaviors of CNTs have usually been explored by two common methods, i.e. continuum mechanics models and atomistic simulations. In continuum mechanics modeling, the CNTs are treated as continuum and homogeneous structures without considering their intrinsic atomic structures. For example, Yoon et al. [13] analyzed the internal vibration of MWCNTs embedded in an external elastic medium by using the multiple-elastic beam model based on the Euler beam assumptions. Based on Eringen's nonlocal elasticity theory [14] and the Euler beam theory, a nonlocal double-walled elastic beam model was developed by Zhang et al. [15] for the free transverse vibrations of double-walled carbon nanotubes. The effect of the small length scale is incorporated in the explicit expression of the natural frequency. Instead of the Euler beam theory, the more refined Timoshenko beam model [16] which allows for the effects of transverse shear deformation and rotary inertia was applied for the free vibration of MWCNTs [17]. Based on the nonlocal elasticity theory and the Timoshenko beam theory, Wang et al. [18] derived the governing equations and boundary conditions for the free vibration of nonlocal Timoshenko beams via Hamiltonian's principle. The exact vibration frequency values of nonlocal Timoshenko beam under various boundary conditions were obtained. Ece and Aydogdu [19] employed the nonlocal Timoshenko beam models to investigate the vibration problem of simply-supported, double-walled CNTs (DWCNTs) under axial load. The influence of the axial load on the natural frequencies of DWCNTs was quantified. Recently, Reddy and Pang [20] reformulated the equations of motion of the Euler and Timoshenko beam theories by using Eringen's nonlocal elasticity theory. The equations of motion are then used to evaluate the static bending, vibration, and buckling responses of CNTs with various boundary conditions. Although the aforementioned beam models are simple and

straightforward to use, the effectiveness of the continuum models in the vibration analysis of CNTs under various conditions has not hitherto been verified by either experiments or atomistic simulations, especially for SWCNTs. Therefore, the applicability of the continuum beam model is still in doubt.

In addition to continuum mechanics models, atomistic simulations have been carried out to explore the vibration characteristics of CNTs. Li and Chou [21] employed the molecular structural mechanics method and model the SWCNT as an equivalent space frame-like structure to examine the feasibility of using SWCNT as a nanoresonator. The predicted fundamental frequencies of clamped-free or clamped SWCNTs were sensitive to dimensions such as length, diameter as well as boundary conditions, but the frequencies are relatively insensitive to chirality of the tubes. Later, Li and Chou [22] extended their work to assess the vibration behavior of MWCNTs by considering the van der Waals interaction between the adjacent tubes. They observed that the frequencies of SWCNTs and DWCNTs were not sensitive to vibration modes, which are in contradiction with the results reported by Cao et al. [24]. By using the same model, Li and Chou [23] assessed the SWCNTs as nanomechanical resonators in the presence of the axial strain or pressure. It was reported that the fundamental frequencies of the SWCNTs decreases with increasing tensile strain, a trend that is in conflict with experimental results of Sazonova et al. [25]. The contradictory results presented by Li and Chou [22, 23] may be due to the simplified molecular structural mechanics model in which only the deformed positions of carbon atoms are computed while neglecting the more important stretching energy term which accounts for the effects such as bond length and angle changes caused by the surrounding atoms [24,26]. A comprehensive molecular dynamics study based on the COMPASS (Condensed-phased Optimized Molecular Potential for Atomistic Simulation Studies) force field and continuum analysis was carried out by Cao et al. [26] to investigate the fundamental frequency shift of deformed clamped-clamped SWCNTs under axial loadings, bending and torsion. The results given by the beam model or the cylindrical shell model are in good agreement with those obtained from MD simulations, provided that the Young's modulus and wall thickness are carefully selected. Yao and Lordi [4] performed MD simulations using the universal force field (UFF) to determine the Young's modulus of various clamped-free SWCNTs from their thermal vibration frequencies by using the frequency equations based on the Euler beam theory.

The atomistic studies performed on the vibration behaviors of CNTs so far are limited. Most of the available continuum beam models for the free transverse vibration of CNTs provide analytical natural frequencies of CNTs under various boundary conditions but the accuracy of the results is questionable. More experimental or atomistic simulations works are required to validate the applicability of the continuum models. The aim of this paper is to provide complete characteristics of vibrating CNTs by performing MD simulations based on the well-known reactive empirical bond-order (REBO) potential [27]. In addition, the applicability and effectiveness of the Timoshenko beam models developed by Wang et al. [18] are assessed by MD simulations vibration results. Furthermore, the effects of length-to-diameter ratio, chirality, bound-

ary conditions, and initial strains on the vibration frequencies are investigated via the MD simulations and Timoshenko beam results. The present comprehensive MD simulations results may also be used to clear the contradictory results presented by Li and Chou [22, 23].

2 Computational model

2.1 Timoshenko beam models

The Timoshenko beam models have been developed in the analysis of free vibration of CNTs by considering the effects of transverse shear deformation and rotary inertia in our previous works [17–20]. These effects neglected in Euler beam models become significant for CNTs with small length-to-diameter ratio those are normally encountered in applications of CNTs such as nanotweezers [28] and nanoprobes [29]. For the sake of completion, a brief overview on the local and nonlocal Timoshenko beam models is presented first [17–20].

The governing equation for a vibrating Timoshenko beam given by Timoshenko [16] is

$$\frac{dM}{dx} = Q - \rho I\omega^2\phi, \tag{2.1}$$

$$\frac{dQ}{dx} = -\rho A\omega^2 w, \tag{2.2}$$

where w is the transverse displacement, ϕ the slope of the beam due to bending deformation alone, x the axial coordinate, I the second moment of area of cross-section, A the cross-sectional area, ρ the mass density per unit volume, ω the circular frequency of the beam, M and Q are the bending moment and shear force, respectively. Based on Erigen's nonlocal elasticity, the bending moment and shear force are expressed as

$$M - (e_0a)^2\frac{d^2M}{dx^2} = EI\frac{d\phi}{dx}, \tag{2.3}$$

$$Q = K_sGA\left(\phi + \frac{dw}{dx}\right), \tag{2.4}$$

where E is the Young's modulus, G the shear modulus, K_s is the shear correction in the Timoshenko beam theory, and e_0a is the scale coefficient that incorporates the small scale effect. Note that a is the internal characteristic length (e.g., lattice parameter, C-C bond length and granular distance) and e_0 is a constant appropriate to each material.

In view of Eqs. (2.3) and (2.4), the governing equations for the vibration of nonlocal Timoshenko beams are given by

$$EI\frac{d^2\phi}{dx^2} - K_sGA\left(\phi + \frac{dw}{dx}\right) + \rho I\omega^2\phi - (e_0a)^2\left(\rho A\omega^2\frac{dw}{dx} + \rho I\omega^2\frac{d^2\phi}{dx^2}\right) = 0, \tag{2.5}$$

$$K_sGA\left(\frac{d\phi}{dx} + \frac{d^2w}{dx^2}\right) + \rho A\omega^2 w = 0. \tag{2.6}$$

Note that the governing equations reduce to those of the local Timoshenko model when the characteristic length a is set to zero. With the boundary conditions, the frequencies can be furnishes by solving the eigenvalue problems. For more details, one can refer to [18].

2.2 Molecular dynamics simulation

Molecular dynamics simulation is a powerful tool for the analysis of nanoscale systems. The basic concept of MD simulations is to simulate the time evolution of a system of atoms. The atoms in the system are treated as point-like masses that interact with one another according to an assumed potential energy. The second-generation REBO potential [27] is adopted to simulate SWCNTs in the present work. This potential can reproduce more accurately the realistic chemical bond properties of hydrocarbon molecules. The second-generation REBO potential relative to its earlier version [30] contains improved analytical functions and an expanded database, which leads to a significantly better description of chemical and mechanical properties for hydrocarbon molecules and diamond [27, 31] that compare reasonably well to first-principles prediction.

The REBO potential is given by the sum of energy over the bonds, i.e.

$$E_b = \sum_i \sum_{j>i} \lfloor V_R(r_{ij}) - \overline{b}_{ij} V_A(r_{ij}) \rfloor, \tag{2.7}$$

where V_R denotes the inter-atomic repulsion (core-core, etc), V_A the attraction from the valence electrons, r_{ij} is the distance between pairs of nearest-neighboring atoms i and j, and $\overline{b}_{ij}$ is the reactive empirical bond order depending on local bonding environment.

In the present vibration simulations, the bonding atomistic interaction in SWCNTs is described by the REBO potential while the non-bonding interaction is neglected to enhance the computational efficiency since it has been proven to have minimal contribution to the total strain energy [32]. The fifth-order Gear's predictor-corrector integration scheme is adopted with a time step size of 1 fs. Since the temperature exerts no effect on the vibration frequency but only it increases the amplitude of vibration, all MD simulations are therefore carried out in a fixed temperature of 1 K maintained by the Berendsen thermostat [33]. The low temperature is chose to avoid the coupled transverse and longitudinal vibrations. After an initial equilibration at the specified temperature, all atoms except those on the fixed end are allowed to vibrate. The histories of the geometric center of the free atoms are recorded for a certain duration (100-1200 ps depending on the size and the boundary conditions of the SWCNTs), and then the vibration frequencies are computed by using the Fast Fourier Transform (FFT) method.

3 Simulation results

Fig. 1 illustrates the three different SWCNTs. It can be seen from Fig. 1 that the CNT resembles a hollow tube structure. In the present study, a set of (5, 5) armchair SWCNTs with different length-to-diameter ratios under clamped-free (CF) and clamped-clamped (CC) boundary conditions are considered. In order to examine the effect of chirality on the vibration frequencies, we simulate SWCNTs with diameters close to the (5, 5) SWCNTs but with different chiral angles. The vibration frequencies of initially pre-stressed SWCNTs under compression and tension are also investigated. All the SWCNTs simulated herein are (5, 5) SWCNTs, unless otherwise stated. The successful application of continuum models into CNTs depends strongly on the selected Young's modulus E and effective thickness h. In order to determine the Young's modulus, one needs to estimate the thickness first. However, the thickness of SWCNTs with a single layer of atoms is ambiguous. Conventionally, the interlayer spacing of graphite $h = 0.34$ nm is taken as the CNT thickness. On the other hand, considerable atomistic simulations in the literature have presented scattered thicknesses for SWCNTs in the range of 0.066-0.34 nm. Huang et al. [34] bypassed atomistic simulations and developed an analytical approach to explain the ambiguity. It is found that the thickness, and therefore elastic moduli, depends on loading type, interatomic potential, nanotube radius and chirality. This dependence explains why the thickness obtained from prior atomistic simulations are scattered.

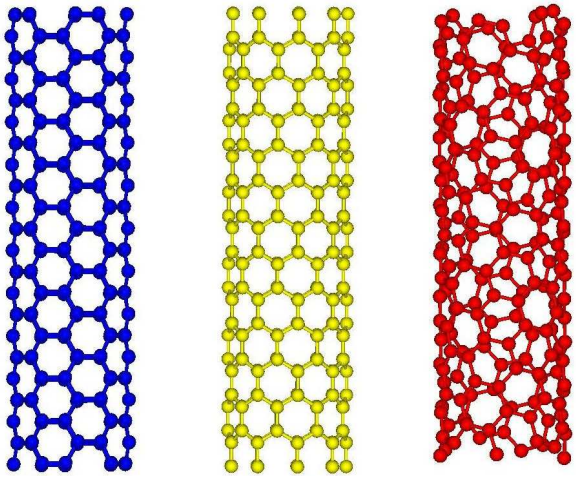

Figure 1: Examples of (5, 5) armchair, (9, 0) zigzag, and (7, 3) chiral nanotubes.

To apply the Timoshenko beam model in the vibration analysis of SWCNTs, it is crucial to determine the Young's modulus and effective thickness first. It is well-known that the natural frequencies f_n for longitudinal vibration of a clamped-free

beam are given by [35]

$$f_n = \frac{(2n-1)}{4L}\sqrt{\frac{E}{\rho}}, \quad n = 1, 2, 3, ..., \tag{3.1}$$

where L is the length of the beam, n the mode of vibration and ρ the mass density of the beam material which is a function of beam thickness h. Herein we use Eq. (3.1) to determine the ratio of E and the mass density for the application of Timoshenko beam model expressed in Eqs. (2.1)-(2.6).

In Eq. (3.1), the ratio of E and the mass density ρ can be determined uniquely and directly from the vibration frequency and the length of the beam by avoiding the definition of the thickness h. Thus the E/ρ ratio may be employed directly in the Timoshenko beam model for the analytical natural frequencies of free transverse vibration. In view of this, MD simulation is first performed to obtain the natural frequency of the longitudinal vibration of a clamped-free SWCNT with a length of 6.92 nm. The E/ρ ratio as calculated from MD simulation is 3.6481×10^8 m^2/s^2. In order to examine the effect of the length on the ratio, a longer tube with a length of 14.4 nm is simulated by MD simulation. The ratio obtained for the longer tube was also found to be identical, indicating the independence of the ratio on the length. Based on the E/ρ ratio, the stiffness is calculated as $Eh = 278.25$ GPa·nm, in good agreement with determined directly from the REBO potential by Huang et al. [34]. Throughout this study, $E/\rho = 3.6481 \times 10^8$ m^2/s^2 is used to calculate the natural frequencies of transverse vibration of the Timoshenko beam model.

3.1 Vibration of clamped-free SWCNTS

Clamped-free (CF) CNTs are often used in both experimental studies [1, 3, 36] and atomistic studies for the prediction of mechanical properties [4, 21–23, 37]. In the present simulations, a set of CF SWCNTs with length-to-diameter ratios varying from 4.67 to 35.34 are considered. Their natural frequencies of transverse vibration are obtained using MD simulations and Timoshenko beam models. The natural frequencies for the first five modes given by the MD simulations are shown in Fig. 2 and Table 1. It can be readily seen that the results generated from MD simulations predict the similar frequency variations as the continuum vibration theory [38], i.e. higher modes produce higher frequencies and the frequency decreases smoothly as the length-to-diameter ratio increases at each mode as shown in Fig. 2. Since the SWCNTs are of almost the same diameter, the inversely proportional relationship between the frequencies and the length-to-diameter ratio indicates that the longer tube is more sensitive to vibration. In addition, the frequencies of the CF SWCNTs obtained by MD simulations based on Brenner's REBO potential are comparable to those given by MD simulations based on COMPASS at room temperature [39]. For example, the frequencies of the first fourth modes for the SWCNTs with calculated by Duan et al. [39] are 0.136, 0.716, 1.676 and 2.736 THz, respectively while the results obtained from the present MD simulations are 0.129, 0.684, 1.630 and 2.704 THz, respectively. It is clearly shown that the

Table 1: Natural frequencies of CF SWCNTs by MD simulations.

L/D	Frequency (THz)				
	1st	2nd	3th	4th	5th
4.67	0.2319	1.1536	2.5909	4.0741	5.4291
6.47	0.1287	0.6836	1.6296	2.7039	3.8210
7.55	0.1000	0.5421	1.3105	2.2842	3.2316
8.28	0.0793	0.4486	1.1139	1.9134	2.7802
10.07	0.0549	0.3143	0.8056	1.4160	2.1057
13.69	0.0305	0.1770	0.4699	0.8606	1.3184
17.30	0.0183	0.1129	0.3052	0.5707	0.8942
20.89	0.0138	0.0794	0.2138	0.4069	0.6414
24.50	0.0092	0.0586	0.1586	0.3052	0.4828
28.07	0.0069	0.0448	0.1207	0.2344	0.3759
31.64	0.0061	0.0351	0.0961	0.1846	0.2991
35.34	0.0046	0.0282	0.0778	0.1495	0.2441

two sets of results are in good agreement with each other and the discrepancy between them can be attributed to the different potential functions used in the MD simulations and somewhat different geometries of the SWCNTs.

The nonlocal Timoshenko model based on Eringen's nonlocal elasticity theory [14] and Timoshenko beam theory was derived by Wang et al. [18] for the free transverse vibration analysis of micro/nano beams. The small scale effect is taken into consideration in the former theory while the effects of transverse shear deformation and rotary inertia are accounted for in the latter theory. By neglecting the small scale effect (i.e. setting the small scale parameter $e_0 = 0$), the nonlocal Timoshenko beam is reduced

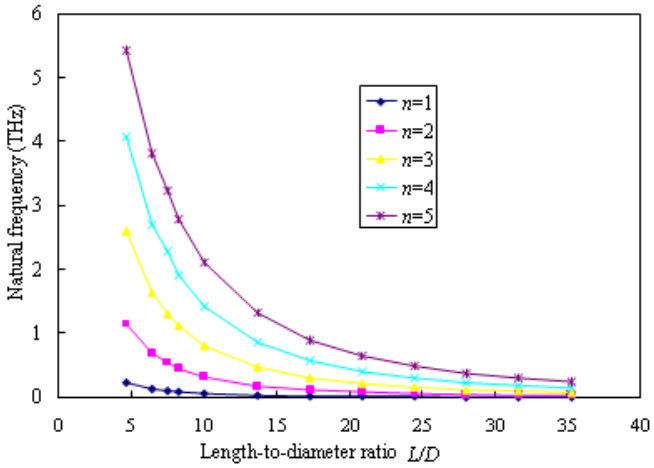

Figure 2: Frequencies of CF SWCNTs for the first five modes against length-to-diameter ratio L/D by MD simulations (curves from top to bottom with decreasing value of n).

to local Timoshenko beam. To make use of the nonlocal Timoshenko beam model as shown in Eq. (2.5) and (2.6) for the theoretical prediction, the magnitude of the small scale parameter must be established. Herein, we adopt the method introduced by Zhang et al. [15] to predict the small scale parameter. It is found that $e_0 = 1.25$ by matching the buckling strains obtained by MD simulations and the continuum shell model reported by Yakobson et al. [6]. Using the ratio $E/\rho = 3.6481 \times 10^8$ m^2/s^2, $e_0 = 1.25$ and the assumed thickness $h = 0.34$ nm or 0.066 nm, the theoretical predictions of the frequencies for the CF SWCNTs are furnished by the local and nonlocal Timoshenko beam models.

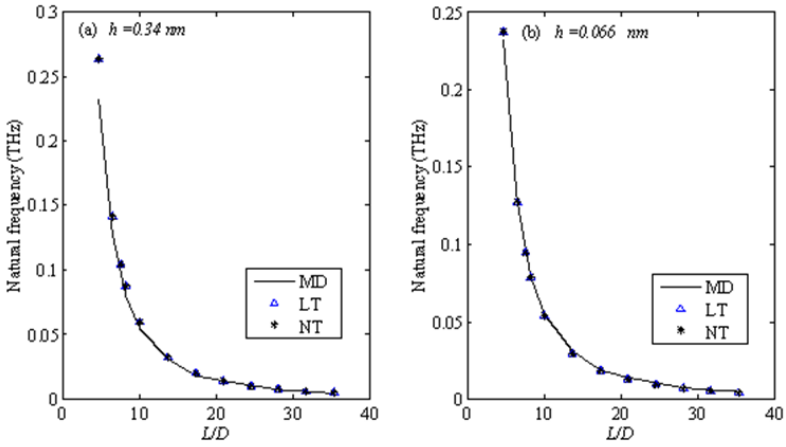

Figure 3: Frequencies of CF SWCNTs for first vibration mode obtained by MD simulations and Timoshenko beam models with $h = 0.34$ nm and $h = 0.066$ nm. (LT-Local Timoshenko beam model; NT-Nonlocal Timoshenko beam model).

To show the effect of the thickness on the theoretical frequencies as calculated by the Timoshenko beam model, two different thicknesses are adopted, i.e. 0.34 nm the interlayer spacing of graphite and 0.066 nm as suggested by Yakobson et al. [6]. The typical frequencies of the first and third mode obtained by MD simulations and Timoshenko beam models based on the local and nonlocal elasticity theory are presented in Tables 2 and 3 and depicted in Figs. 3 and 4, respectively. The theoretical results are compared with those by MD simulations and the percentage difference δ is given. From Table 2, it can be observed that both the local and nonlocal Timoshenko beam models with $h = 0.34$ nm produce higher frequencies than those obtained from MD simulations. The largest percentage of difference is 0.1376 and it is associated with the shortest tube of $L/D = 4.67$. The consideration of small scale effect in nonlocal Timoshenko beam model leads to relatively better results than its local counterpart in the case for $h = 0.34$ nm. However, with the smaller thickness $h = 0.066$ nm, both Timoshenko beam models underestimated the frequencies. Similarly, it is found from Table 3 that both local and nonlocal Timoshenko beams also produce higher frequen-

Table 2: Frequencies of CF SWCNTs for first vibration mode obtained by MD simulations and Timoshenko beam models with $h = 0.34$ nm and $h = 0.066$ nm.

L/D	MD	$h = 0.34$ nm				$h = 0.066$ nm			
		LT^*	$\delta\%$	NT^*	$\delta\%$	LT	$\delta\%$	NT	$\delta\%$
4.67	0.23193	0.26357	13.64	0.26386	13.76	0.23711	2.23	0.23739	2.35
6.47	0.12872	0.14134	9.81	0.14143	9.88	0.12721	-1.17	0.12730	-1.11
7.55	0.09766	0.10491	7.43	0.10496	7.48	0.09444	-3.29	0.09449	-3.25
8.28	0.07935	0.08760	10.40	0.08763	10.44	0.07885	-0.62	0.07888	-0.58
10.07	0.05493	0.05960	8.50	0.05962	8.54	0.05366	-2.31	0.05367	-2.29
13.69	0.03052	0.03248	6.43	0.03248	6.44	0.02924	-4.17	0.02924	-4.17
17.30	0.01831	0.02041	11.44	0.02041	11.45	0.01837	0.33	0.01837	0.34
20.89	0.01221	0.01401	14.77	0.01401	14.77	0.01261	3.30	0.01261	3.31
24.50	0.00916	0.01020	11.32	0.01020	11.32	0.00918	0.27	0.00918	0.28
28.07	0.00690	0.00777	12.65	0.00777	12.65	0.00699	1.43	0.00700	1.43
31.64	0.00610	0.00612	0.20	0.00612	0.22	0.00551	-9.77	0.00551	-9.76
35.34	0.00458	0.00491	7.24	0.00491	7.24	0.00442	-3.45	0.00442	-3.45

$^*LT$-Local Timoshenko beam model; NT-Nonlocal Timoshenko beam model.

cies for the third mode with $h = 0.34$ nm than those obtained by MD simulations. The effect of small scale parameter is significant for stocky SWCNTs with small length-to-diameter ratio L/D but negligible for slender SWCNTs. In the case of $h = 0.066$ nm, both beams give lower frequencies than MD simulations. The first and third mode frequencies against L/D are also shown in Figs. 3 and 4, respectively. It is clearly demonstrated that the thickness of CNTs plays a significant role in the application of continuum mechanics models, as well as the Young's modulus. The thickness of 0.066 nm adopted in the beam model can produce much better results than 0.34 nm. Recently an attempt was made by Huang et al. [34] to derive the thickness of graphite and SWCNTs directly from the interatomic potentials but the analytic approach fails to give a unique thickness for SWCNTs. The thickness of SWCNTs is in the range of 0.06 0.09 nm. More works are needed to address this issue.

Despite the differences between the results given by the Timoshenko beam model and MD simulations as shown in Tables 2 and 3, it may be reasonable to conclude that the Timoshenko beam model with properly chosen Young's modulus E and thickness h can reproduce frequencies that are in reasonable agreement with those by MD simulations. For the CF SWCNTs, the adoption of thickness $h = 0.066$ nm can reproduce much better results than 0.34 nm with the largest percentage of difference 9.77% and 6.22% for the first and third vibration modes, respectively.

3.2 Vibration of clamped-clamped SWCNTS

In applications as micro- or nanostrain sensors and micro-oscillators, the CNT sensor is generally clamped at both ends [40]. Considerable atomistic simulations have been performed on the clamped-clamped (CC) SWCNTs [21–23, 26]. In this section, the set of clamped-clamped (CC) SWCNTs is simulated by Timoshenko beam models and MD simulations for their vibration frequencies. Again the frequencies of the CC SWC-

Table 3: Frequencies of CF SWCNTs for third vibration mode obtained by MD simulations and Timoshenko beam models with $h = 0.34$ nm and $h = 0.066$ nm.

L/D	MD	$h = 0.34$ nm				$h = 0.066$ nm			
		LT	$\delta\%$	NT	$\delta\%$	LT	$\delta\%$	NT	$\delta\%$
4.67	2.59094	2.80678	8.33	2.71884	4.94	2.51329	-3.00	2.43957	-5.84
6.47	1.62964	1.76408	8.25	1.72720	5.99	1.58080	-3.00	1.54924	-4.93
7.55	1.31226	1.39518	6.32	1.37146	4.51	1.25114	-4.66	1.23065	-6.22
8.28	1.11389	1.20559	8.23	1.18758	6.62	1.08154	-2.90	1.06591	-4.31
10.07	0.80556	0.87329	8.41	0.86354	7.20	0.78413	-2.66	0.77558	-3.72
13.69	0.46997	0.51139	8.81	0.50791	8.07	0.45967	-2.19	0.45659	-2.85
17.30	0.30518	0.33334	9.23	0.33182	8.73	0.29980	-1.76	0.29845	-2.20
20.89	0.21362	0.23369	9.39	0.23294	9.04	0.21025	-1.58	0.20958	-1.89
24.50	0.15862	0.17234	8.65	0.17193	8.39	0.15510	-2.22	0.15426	-2.75
28.07	0.12069	0.13243	9.73	0.13219	9.53	0.11920	-1.24	0.11898	-1.42
31.64	0.09613	0.10491	9.13	0.10473	8.95	0.09443	-1.77	0.09429	-1.92
35.34	0.07782	0.08456	8.66	0.08456	8.66	0.07611	-2.19	0.07602	-2.31

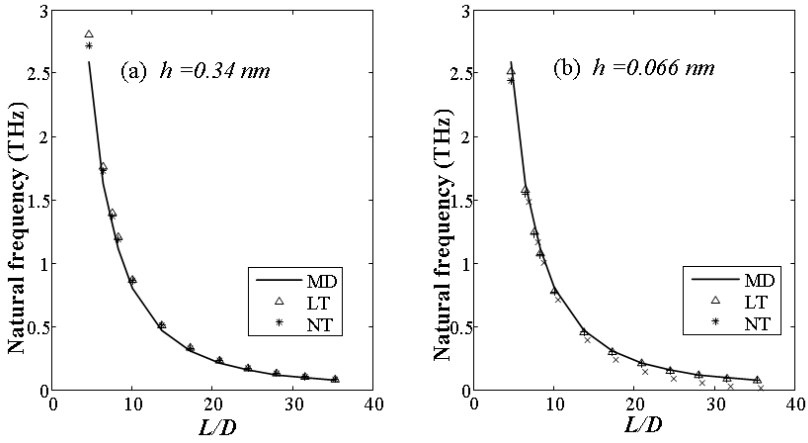

Figure 4: Frequencies of CF SWCNTs for third vibration mode obtained by MD simulations and Timoshenko beam models with $h = 0.34$ nm and $h = 0.066$ nm.

NTs obtained by MD simulations based on Brenner's REBO potential are comparable to those given by MD simulations based on COMPASS force field [24]. The frequencies of the first fourth modes for the CC (5,5) SWCNTs calculated by Cao et al. [24] are 0.037, 0.104, 0.208 and 0.328 THz while the results obtained from the present MD simulations are 0.036, 0.108, 0.185 and 0.326 THz, respectively. It is observed that the two sets of results are in good agreement with each other. With the view to compare the results with those of CF SWCNTs, the same (5, 5) armchair SWCNT is used with similar length-to-diameter ratios L/D. The typical first and third mode frequencies obtained from MD simulations are shown in Fig. 5 and Fig. 6, respectively and compared with those obtained by using the Timoshenko beam models with thicknesses $h = 0.34$ nm

Table 4: Frequencies of CC SWCNTs for first vibration mode obtained by MD simulations and Timoshenko beam models with $h = 0.34$ nm and $h = 0.066$ nm.

L/D	MD	$h = 0.34$ nm				$h = 0.066$ nm			
		LT	$\delta\%$	NT	$\delta\%$	LT	$\delta\%$	NT	$\delta\%$
4.86	1.06812	1.14229	6.94	1.13240	6.02	1.01126	-5.32	1.00309	-6.09
6.67	0.64697	0.69764	7.83	0.69347	7.18	0.62092	-4.02	0.61738	-4.57
8.47	0.43335	0.46628	7.60	0.46428	7.14	0.41641	-3.91	0.41469	-4.31
10.26	0.30518	0.33214	8.83	0.33109	8.49	0.29726	-2.59	0.29634	-2.90
13.89	0.18311	0.18999	3.76	0.18963	3.56	0.17044	-6.92	0.17012	-7.09
17.49	0.11597	0.12255	5.67	0.12239	5.54	0.11007	-5.09	0.10993	-5.20
21.06	0.07629	0.08555	12.14	0.08548	12.04	0.07690	0.80	0.07684	0.71
24.66	0.05798	0.06285	8.40	0.06281	8.33	0.05652	-2.52	0.05649	-2.58
28.31	0.04578	0.04796	4.77	0.04793	4.71	0.04314	-5.76	0.04312	-5.81
31.85	0.03662	0.03800	5.85	0.03798	5.80	0.03419	-4.76	0.03417	-4.80
35.53	0.03052	0.03062	0.34	0.03061	0.30	0.02755	-9.71	0.02754	-9.74

Table 5: Frequencies of CC SWCNTs for third vibration mode obtained by MD simulations and Timoshenko beam models with $h = 0.34$ nm and $h = 0.066$ nm.

L/D	MD	$h = 0.34$ nm				$h = 0.066$ nm			
		LT	$\delta\%$	NT	$\delta\%$	LT	$\delta\%$	NT	$\delta\%$
4.86	3.75061	3.94940	5.30	3.78132	0.82	3.48932	-6.96	3.35429	-10.56
6.67	2.51110	2.63529	5.31	2.55534	2.11	2.33383	-6.74	2.26795	-9.37
8.47	1.79443	1.89364	5.53	1.84985	3.09	1.68149	-6.29	1.64480	-8.34
10.26	1.34280	1.42670	6.25	1.40065	4.31	1.26992	-5.43	1.24780	-7.07
13.89	0.83620	0.88150	5.42	0.87088	4.15	0.78744	-5.83	0.77825	-6.93
17.49	0.55540	0.59514	7.15	0.59009	6.25	0.53286	-4.06	0.52844	-4.85
21.06	0.38760	0.42745	10.28	0.42478	9.59	0.38333	-1.10	0.38097	-1.71
24.66	0.29600	0.32003	8.12	0.32073	8.36	0.28727	-2.95	0.28592	-3.41
28.31	0.23193	0.24741	6.67	0.24649	6.28	0.22222	-5.44	0.22141	-5.78
31.85	0.18310	0.19780	8.03	0.19721	7.71	0.17776	-2.92	0.17723	-3.20
35.53	0.15260	0.16051	5.19	0.16012	4.93	0.14429	-5.44	0.14394	-5.67

and $h = 0.066$ nm. The magnitudes of the first and third mode frequencies given by the beam models as well as MD simulations are presented in Tables 4 and 5, respectively. It can be seen from Tables 2 and 4 that the L/D of the set of CC SWCNTs is slightly different from that of CF SWCNTs due to the influence of the boundary conditions. For a similar L/D, the frequencies of CC SWCNTs given by MD simulations are higher than those of its CF counterpart due to the boundary condition. The relationship between L/D and frequencies, the effect of thickness used in Timoshenko beam model, the effect of boundary conditions in MD simulations, and the effect of the small scale parameter on the frequencies of CC SWCNTs are similar to those addressed above for CF SWCNTs. Again, the Timoshenko beam models with or without small scale effects can provide satisfactory frequencies for the CC SWCNTs since they compare well with those given by MD simulations.

Based on the theoretical and atomistic predictions of frequencies for CC and CF SWCNTs, it is clearly demonstrated that the Timoshenko beam models can be appli-

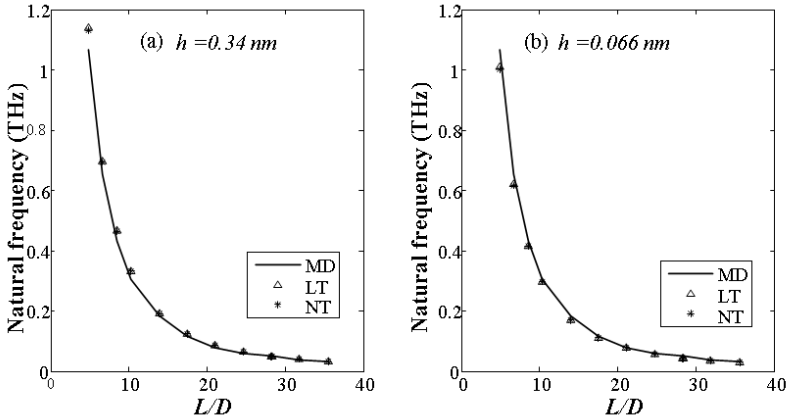

Figure 5: Frequencies of CC SWCNTs for first vibration mode obtained by MD simulations and Timoshenko beam models with $h = 0.34$ nm and $h = 0.066$ nm.

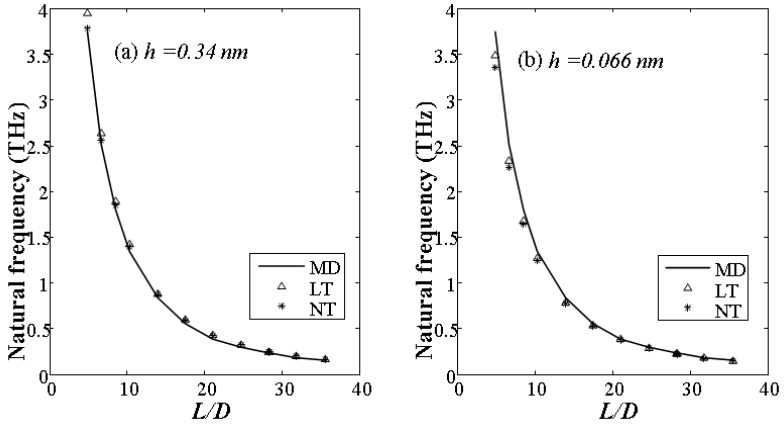

Figure 6: Frequencies of CC SWCNTs for third vibration mode obtained by MD simulations and Timoshenko beam models with $h = 0.34$ nm and $h = 0.066$ nm.

cable to the vibration analysis especially when the small thickness $h = 0.066$ nm is used.

3.3 Effect of chirality

As shown in previous atomistic simulations [11] on a set of SWCNTs with various chiral angles under compression, chirality of SWCNTs plays a significant role in the buckling behaviors of CNTs. This finding urges us to explore further the possible role of chirality in the vibration behaviors of SWCNTs.

Five CF SWCNTs with various chiral angles are simulated by MD simulations.

Table 6: Frequencies of CF SWCNTs with different chiral angles.

SWCNTs	*CA	Frequency (THz)				
		1st	2nd	3rd	4st	5st
(9,0)	0.00	0.05493	0.30518	0.76904	1.31836	1.90430
(8,2)	10.89	0.05493	0.29907	0.75684	1.30615	1.91040
(7,3)	17.00	0.05493	0.29907	0.76904	1.34277	1.98364
(6,4)	23.41	0.05493	0.31128	0.78735	1.38550	2.02367
(5,5)	30.00	0.05493	0.31128	0.80556	1.41602	2.10571

*CA - Chiral angle (degree).

The five chiral indices, namely, (5,5), (6,4), (7,3), (8,2) and (9,0), are chosen so that the nanotubes have approximately the same diameters and tube lengths. The length-to-diameter ratio L/D results in a value of 10.07. Under otherwise identical conditions, the effect of chirality of SWCNTs can be identified.

The vibration frequencies of the SWCNTs obtained from MD simulations are shown in Table 6. From Table 6, it is clearly seen that the fundamental frequencies of the SWCNTs are same, i.e., independent of the magnitude of chiral angles. This means that chirality has no effect on the fundamental frequency of SWCNTs. This observation is in agreement with some findings reported by Li and Chou [21] using molecular structural model. As the vibration modes increase, the effect on frequency becomes distinct. In addition, larger chiral angles would lead to an increase in frequency, and this increase is amplified at higher vibration modes. For example, the percentage differences between the smallest and largest frequencies at the higher vibration modes (from second to fifth) are 3.923%, 6.048%, 7.759% and 9.565%, respectively. The percentage difference is found to increase with higher vibration modes. Since the SWCNTs have similar diameters and lengths, the frequencies calculated by using the Timoshenko beam models are expected to be close. In other words, Timoshenko beam model fails to capture the effect of chirality. However, it is demonstrated that the neglect of chirality effect in the simple Timoshenko beam model only lead to 9.565% difference for the fifth vibration mode and even a smaller difference for lower modes. This neglect is acceptable from a practical viewpoint. In sum, the Timoshenko beam model cannot capture the effect of chirality but it can predict vibration frequencies up to the fifth vibration mode within an acceptable error of 10%.

In summary, chirality has no effect on the fundamental frequencies but it influences the frequencies of higher vibration modes. SWCNTs with larger chiral angles have higher frequencies except for the first mode of vibration. The Timoshenko beam model can be employed for the prediction of the fundamental frequencies of chiral CNTs accurately since the fundamental frequencies are independent of chiral angles. In addition, the Timoshenko beam model can also been used for the prediction of other frequencies of higher vibration modes with acceptable errors.

3.4 Effect of initial strain

The resonant frequency of CNTs is very sensitive to the external loads. This is the basic principle of CNTs-based resonant strain sensor. The key issue of strain sensing is to find the relationship between the resonant frequency of the CNTs and the applied stress on the tubes. Therefore it is important to understand the vibration behaviors of the CNTs in the presence of initial strains (compressive or tensile in nature) before fulfilling CNTs potential as nano-sensors.

In this section, MD simulations are performed on CC SWCNTs of moderate length with length-to-diameter $L/D = 13.89$ under either compressive or tensile strains to study their sensitivity to the imposed strain. By considering the initial strain in the vibration governing equations of the nonlocal Timoshenko beam model, the analytical frequencies can be calculated and compared with those given by MD simulations. The fundamental vibration frequency is one of the most basic CNT mechanical properties. The two papers in the literature on the strain sensing of CNTs were focus on the fundamental frequency at small strain level ($< 1.3\%$) [23, 26]. Herein we explore the dependence of the fundamental frequency of CC SWCNTs on the initial strain by using MD simulations and nonlocal Timoshenko beam models with thicknesses of 0.34 nm and 0.066 nm. The sensitivity of the CNTs to initial strain is checked by applying small strains ($< 1.5\%$) to the CNTs.

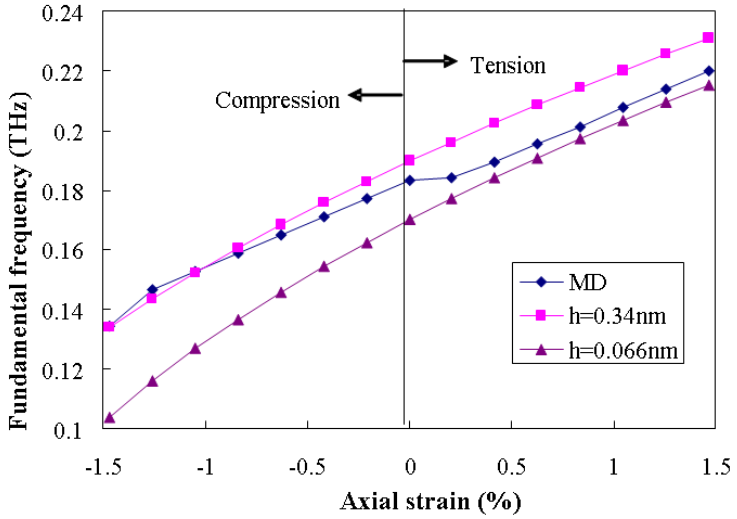

Figure 7: Variations of fundamental frequencies with respect to initial strains.

The typical fundamental frequencies given by MD simulations and nonlocal Timoshenko beam models with the same mechanical parameters mentioned above are depicted in Fig. 7. It is noted that negative strains denote compression while positive ones tension. It is readily observed from Fig. 7 that the presence of a compressive initial strain leads to a reduction in the frequencies whereas a tensile initial strain in-

creases the frequencies, which is in agreement with the prediction of continuum vibration theory [38]. However, this conflicts with the observation of Li and Chou [23]. The application of different thicknesses in nonlocal Timoshenko beam model results in two different sets of frequencies and the larger thickness of 0.34 nm leads to higher frequencies at different initial strain levels as shown in Fig. 7. This indicates the crucial role that the thickness plays in continuum mechanics models. Fig. 7 shows that the frequencies given by the MD simulations are between the two sets of results given by Timoshenko beam model using thickness of 0.34 nm and 0.066 nm, respectively. It is also observed from Fig. 7 that the frequencies under tension using thickness of 0.066 nm are close to those by MD simulations while the frequencies under compression using thickness of 0.34 nm instead agree well with those by MD simulations. This indicates that the thickness of SWCNTs depends on the type of loading, in agreement with the conclusion reached by Huang et al. [34].

4 Conclusions

The vibration behaviors of CF and CC SWCNTs are extensively investigated by means of MD simulations based on Brenner's REBO potential and the effectiveness of the Timoshenko beam models are assessed. With properly chosen parameters, the Timoshenko beam models can reproduce satisfactory frequencies that are in reasonable agreement with those obtained by MD simulations. Through the comparison, it is found that the smaller thickness of 0.066 nm in the Timoshenko beam model could lead to better results than 0.34 nm in most of the cases studied in the present work. The effects of the length-to-diameter ratio, boundary conditions, chirality and initial strains on the frequencies are also examined via MD simulations and Timoshenko beam models. Based on MD simulation results, it is found that the frequencies decrease with increasing tube lengths and that higher vibration modes possess higher frequencies. The presence of the chirality has no influence on the fundamental frequencies but has appreciable effects on the frequencies at higher vibration modes. The introduction of initial compressive strains leads to a reduction of the frequencies while the initial tensile strains lead to an increase of the frequencies.

References

[1] M. M. J. Treacy, T. W. Ebbesen and J. M. Gibson, *Exceptionally high Young's modulus observed for individual carbon nanotubes*, Nature, 381 (1996), pp. 678-680.

[2] A. Krishnan, E. Dujardin, T. W. Ebbesen, P. N. Yianilos and M. M. J. Treacy, *Young's modulus of single-walled nanotubes*, Phys. Rev. B, 58 (1998), pp. 14013-19.

[3] P. Poncharal, Z. L. Wang, D. Ugarte and W. A. de Heer, *Electrostatic deflection and electromechanical resonators*, Science, 283 (1999), pp. 1513-6.

[4] Q. Zhao, Z. H. Gan and O. K. Zhuang, *Electrochemical sensors based on carbon nanotubes, Electroanalysis*, Electroanal., 14 (2002), pp. 1609-13.

[5] N. YAO AND V. LORDI, *Young's modulus of single-walled carbon nanotubes*, J. Appl. Phys., 84 (1998), pp. 1939-43.
[6] B. I. YAKOBSON, C. J. BRABEC AND J. BERNHOLC, *Nanomechanics of carbon tubes: Instabilities beyond linear response*, Phys. Rev. Lett., 76 (1996), pp. 2511-2514.
[7] C. F. CORNWELL AND L. T. WILLE, *Elastic properties of single-walled carbon nanotubes in compression, Solid State*, Commun., 101 (1997), pp. 555-558.
[8] M. J. BUEHLER, J. KONG AND H. J. GAO, *Deformation mechanism of very long single-wall carbon nanotubes subject to compressive loading*, J. Eng. Mate. Tech., 126 (2004), pp. 245-249.
[9] B. I. YAKOBSON, M. P. CAMPBELL, C. J. BRABEC AND J. BERNHOLC, *High strain rate fracture and C-chain unraveling in carbon nanotubes*, Comp. Mater. Sci., 8(1997), pp. 341-348.
[10] G. X. CAO AND X. CHEN, *Buckling of single-walled carbon nanotubes upon bending: Molecular dynamics simulations and finite element method*, Phys. Rev. B, 73 (2006), 155435.
[11] Y. Y. ZHANG, V. B. C. TAN AND C. M. WANG, *Effect of chirality on buckling behavior of single- walled carbon nanotubes*, J. Appl. Phys., 100 (2006), 074304.
[12] Y. Y. ZHANG, V. B. C. TAN AND C. M. WANG, *Effect of strain rate on the buckling behavior of single- and double-walled carbon nanotubes*, Carbon, 45 (2007), pp. 514-523.
[13] J. YOON, C. Q. RU AND A. MIODUCHOWSKI, *Vibration of an embedded multiwall carbon nanotube*, Compos. Sci. Technol., 63(2003), pp. 1533-42.
[14] A. C. ERINGEN, *Nonlocal polar elastic continua*, Int. J. Eng. Sci., 10 (1972), pp. 1-16.
[15] Y. Q. ZHANG, G. R. LIU AND X. Y. XIE, *Free transverse vibrations of double-walled carbon nanotubes using a theory of nonlocal elasticity*, Phys. Rev. B, 71 (2005), pp. 195404.
[16] S. TIMOSHENKO, *Vibration Problems in Engineering*, Wiley, New York, 1974.
[17] C. M. WANG, V. B. C. TAN AND Y. Y. ZHANG, *Timoshenko beam model for vibration analysis of multi-walled carbon nanotubes*, J. Sound. Vib., 294 (2006), pp. 1060-1072.
[18] C. M. WANG, Y. Y. ZHANG AND X. Q. HE, *Vibration of nonlocal Timoshenko beams*, Nanotechnology, 18 (2007), pp. 105401.
[19] M. C. ECE AND M. AYDOGDU, *Nonlocal elasticity effect on vibration of in-plane loaded double-walled carbon nanotubes*, Acta Mechanica, 190 (2007), pp. 185-195.
[20] J. N. REDDY AND S. D. PANG, *Nonlocal continuum theories of beams for the analysis of carbon nanotubes*, J. Appl. Phys., 103 (2008), pp. 023511.
[21] C. Y. LI, T. W. CHOU, *Single-walled carbon nanotubes as ultrahigh frequency nanomechanical resonators*, Phys. Rev. B, 68 (2003), pp. 073405.
[22] C. Y. LI AND T. W. CHOU, *Vibrational behaviors of multiwalled-carbon-nanotube-based nanomechanical resonators*, Appl. Phys. Lett., 84 (2003), pp. 121-123.
[23] C. Y. LI AND T. W. CHOU, *Strain and pressure sensing using single-walled carbon nanotubes*, Nanotechnology, 15 (2004), pp. 1493-1496.
[24] G. X. CAO, X. CHEN AND J. W. KYSAR, *Thermal vibration and apparent thermal contraction of single-walled carbon nanotubes*, J. Mech. Phys. Solids, 54 (2006), pp. 1206-1236.
[25] V. SAZONOVA, Y. YAISH, H. USTUNEL, D. ROUNDY, T. A. ARIAS AND P. L. MCEUEN, *A tunable carbon nanotube electromechanical oscillator*, Nature, 431 (2004), pp. 284.
[26] G. X. CAO, X. CHEN AND J. W. KYSAR, *Strain sensing of carbon nanotubes: Numerical analysis of the vibrational frequency of deformed sing-wall carbon nanotubes*, Phys. Rev. B, 72 (2005,) pp. 195412.
[27] D. W. BRENNER, O. A. SHENDEROVA, J. A. HARRISON, S. J. STUART, B. NI AND S. B. SINNOTT, *A second-generation reactive empirical bond order (REBO) potential energy expression for hydrocarbons*, J. Phys.: Condens. Matter., 14 (2002), pp. 783-802.
[28] P. KIM AND C. M. LIEBER, *Nanotube nanotweezers*, Science, 286 (1999), pp. 2148-2150.

[29] E. S. SNOW, P. M. CAMPBEL AND J. P. NOVAK, *Single-wall nanotubes atomic force microscope probes*, Appl. Phys. Lett., 80 (2002), pp. 2002-2004.
[30] D. W. BRENNER, *Empirical potential for hydrocarbons for use in simulation the chemical vapor deposition of diamond films*, Phys. Rev. B, 42 (1990), pp. 9458.
[31] O. A. SHENDEROVA, D. W. BRENNER, A. OMELTCHENKO, X. SU, L. H. YANG, *Atomistic modeling of the fracture of polycrystalline diamond*, Phys. Rev. B, 61 (2000), pp. 3877.
[32] Y. Y. ZHANG, C. M. WANG AND V. B. C. TAN, *Examining the effects of wall numbers on buckling behavior and mechanical properties of MWCNTs based on MDS results*, J. Appl. Phys., 103 (2008), pp. 053505.
[33] H. J. C. BRENDSEN, J. P. M. POSTMA, W. F. VAN GUNSTEREN, A. DINOLA AND J. R. HAAK, *Molecular dynamics with coupling to an external bath*, J. Chem. Phys., 81 (1984), pp. 3684-3690.
[34] Y. HUANG, J. WU AND K. C. HWANG, *Thickness of graphene and single-wall carbon nanotubes*, Phys. Rev. B, 74 (2006), pp. 245413.
[35] D. J. INMAN, *Engineering Vibration*, Prentice Hall, 2000.
[36] S. T. PURCELL, P. VINCENT, C. JOURNET AND V. T. BINH, *Tuning of nanotube mechanical resonances by electric field pulling*, Phys. Rev. Lett., 89 (2002), pp. 276103.
[37] H. JIANG, M. F. YU, B. LIU AND Y. HUANG, *Intrinsic energy loss mechanisms in a clamped-free carbon nanotube beam oscillator*, Phys. Rev. Lett., 93 (2004), pp. 185501.
[38] S. S. RAO, *Mechanical Vibrations*, Prentice-Hall, Englewood Cliffs, NJ, 2002.
[39] W. H. DUAN, C. M. WANG AND Y. Y. ZHANG, *Calibration of nonlocal scaling effect parameter for free vibration of carbon nanotubes by molecular dynamics*, J. Appl. Phys., 101 (2007), pp. 024305.
[40] P. HAUPTMANN, *Resonant sensors and applications*, Sensors and Actuators A-Physical, 26 (1991), pp. 371-377.